Removal Efficiency of Textile Dyes from Aqueous Solutions Using Calcined Waste of Eggshells as Eco-friendly Adsorbent: Kinetic and Thermodynamic Studies

R. Slimani,[a] I. El Ouahabi,[b] S. Benkaddour,[b] H. Hiyane,[b] M. Essoufy,[a] Y. Achour,[c] S. El Antri,[b] S. Lazar,[b,*] and M. El Haddad[c]

[a]Laboratory of Spectroscopy, Molecular Modeling, Materials, Nanomaterials, Water & Environment-CERNE2D, Faculty of Sciences, Mohammed V University in Rabat, BP 1014RP, Rabat, Morocco

[b]Laboratory of Biochemistry, Environment &Agroalimentary URAC36, Faculty of Sciences and Techniques, Hassan II University of Casablanca, BP 146, 20650, Mohammedia, Morocco

[c]Laboratory of Analytical & Molecular Chemistry, Faculty Poly-Disciplinary of Safi, University of Cadi Ayyad, BP4162, 46000 Safi, Morocco

This research investigates the removal of textile dyes (Rhodamine B and Alizarin Red S) from aqueous solution by a low-cost adsorbent prepared from eggshell waste. Batch adsorption experiments were conducted in order to determine the effect of different parameters such as pH, dye concentration, contact time, adsorbent dosage, particle size, and temperature. The best correlation was found by Langmuir model, and the maximum adsorption capacity was 175.58 mg g^{-1} for Rhodamine B and 156.56 mg g^{-1} for Alizarin Red S. Thermodynamic studies showed that the adsorption of Rhodamine B and Alizarin Red S were feasible, spontaneous, and exothermic in nature. Regeneration study conducted to test the reusability (five cycles) and comparison of adsorption capacities of Rhodamine B and Alizarin Red S showed that calcined eggshell adsorbent could potentially be used for the removal of dyes from aqueous solutions.

Keywords:
calcined eggshells, dye, adsorption, kinetics, isotherms

Introduction

Dyes are widely used in different manufacturing industries, of which the textile industry is their largest consumer, and a large producer of dye-loaded wastewater. During the dyeing process, about 10–15 % of unfixed dye is lost in the water, which comes out as a colored effluent from the industries[1]. Additionally, dyes are thermally stable compounds that are light-resistant and non-biodegradable because of their complex molecular structures. Most dyes and their degradation products cause serious damage to the ecosystem and biological life due to their toxicity[2,3]; therefore, it is necessary to remove dyes from the wastewater to protect the eco-system and human health. There are various studies on the physicochemical strategies for removal of dyes from aqueous systems; and among the available methods, adsorption is a well-known separation technique in terms of initial cost, simplicity, design, ease of separation, and ability to treat dyes in a more concentrated form[4].

Activated carbon is the most preferred adsorbent for dye removal because of its excellent adsorption ability. However, an extensive usage of activated carbon is restricted because of its high cost. Alternative adsorbents are required to be of low cost when minimal processing is required, abundant in nature, or derived from an industry by-product[5]. Some of the potential alternative adsorbents studied by a number of researchers include *Cerastoderma lamarcki* shell[6], watermelon seeds[7], calcined cow leather[8], animal bones[9], mussel shells[10], *Ensissiliqua* shell[11], and conch shells[12].

Rhodamine B is a highly water soluble, cationic dye of the xanthene class, and widely used in biological, analytical and optical sciences. It is reported that Rhodamine B is harmful to the environment[13,14]. Alizarin Red S is an anionic dye of the anthraquinon class, which is widely used in woven fabrics, wool, and cotton textiles[15,16]. Many re-

*Corresponding author at: E-mail address:
SAID.LAZAR@univh2c.ma / lazar_said@yahoo.fr (S. Lazar)
Tel : +212 5 23 31 47 05/Fax : +212 5 23 31 53 53

searchers have been interested in the removal of these dyes from aqueous solutions; and in fact, *Raphiahookeri* fruit's epicarp removed Rhodamine B from an aqueous solution with a maximum adsorption capacity of 666.67 mg g^{-1} [17]. Zamouche *et al.* reported the adsorption of Rhodamine B onto cedar cone by studying the effect of calcination and chemical activation[18]. Adsorption of Rhodamine B has also been studied on iron-pillared bentonite, and the maximum monolayer adsorption capacity of 98.62 mg g^{-1} [19] was attained. Mustard husk removed Alizarin Red S with a multilayer adsorption mechanism[20], which was also achieved on olive stone by-product giving 16 mg g^{-1} as adsorption capacity[21]. Roosta *et al.* developed an Alizarin Red S adsorption process from aqueous solution onto gold nanoparticles by the application of ultrasound, giving a high adsorption capacity of 123.4 mg g^{-1} [22].

The aim of the present study was to evaluate and investigate the performance of a newly developed adsorbent, i.e., eggshell powder. This adsorbent was chosen according to its daily presence in domestic waste worldwide. It is an abundant waste, and currently not used in any way. It can be thermally activated for the rapid removal and fast adsorption of Rhodamine B and Alizarin Red S from aqueous solutions with initial dye concentration (20 mg L^{-1} – 50 mg L^{-1}), which exceeds the actual discharge limit rates. The developed adsorbent was well characterized using various analytical techniques, such as Fourier transform infrared spectroscopy (FTIR), X-ray diffraction (XRD), and scanning electron microscopy (SEM). The impact of several influential parameters, such as solution pH, initial dye concentration, contact time, adsorbent dosage, and temperature were well investigated and optimized using batch adsorption study. Moreover, kinetics and thermodynamics of adsorption of Rhodamine B and Alizarin Red S were studied and discussed.
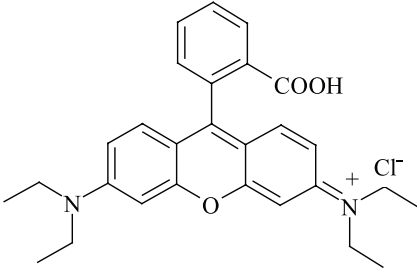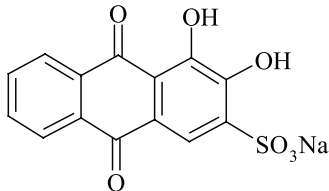
Materials and methods

Chemicals

All chemicals used were of analytical reagent grade and used without further purification. All solutions were prepared using double distilled water. Rhodamine B and Alizarin Red S dyes were supplied by Sigma Aldrich. Some of the data on both dyes are listed in Table 1. The stock solutions of Rhodamine B and Alizarin Red S dyes (1 g L^{-1}) were prepared by dissolving the required amount of dyes in distilled water.

Preparation of calcined eggshell adsorbent

Preparation of the obtained calcined eggshell (CES) absorbent was achieved by collecting eggshell waste from a restaurant. Firstly, the eggshells were washed several times with tap water and distilled water, and then left in open air for several hours, and dried for another 12 hours at 100 °C. The product was then crushed into small pieces, powdered, and calcined at 900 °C for 2 hours. The resulting material was washed with distilled water several times and dried overnight at 105 °C, In addition, the residue was chopped and the fraction of size range 75 – 100 μm was collected. The powder was then dried overnight at 105 °C, and calcined at a heating rate of 2 °C min^{-1} to 400 °C, and maintained at this temperature for 4 hours. The powder was then cooled and stored in a dry place.

T a b l e 1 – *Data of Rhodamine B and Alizarin Red S as studied dyes*

Usual name	Chemical structure	CI Number	Molecular weight (g mol^{-1})	λ_{max} (nm)
Rhodamine B		45 170	479.01	554
Alizarin Red S		58 005	342.26	520

Instrumentation

The measurements of the dye concentration were performed using a molecular absorption UV-Vis spectrophotometer (BioMate6, England) using a quartz cuvette of 1.0 cm at the wavelength attributed to the maximum absorbance of each dye (see Table 1). Chemical composition of CES adsorbent was studied by X-ray fluorescence (WD-XRF). The Fourier-transform infrared spectra (FTIR) were collected by a Nicolet 5700 FT-IR spectrometer on samples prepared as KBr pellets, in a spectral range of 400 – 4000 cm^{-1}. The polycrystalline sample of CES adsorbent was finely ground in an agate mortar with a pestle, and filled into a 0.5-mm borosilicate capillary prior to being mounted and aligned on an Empyrean Panalytical powder diffractometer, using Cu K$_\alpha$ radiation (λ = 1.54056 Å). Three repeated measurements were collected at ambient temperature (22 °C) in the $10° < 2\theta < 60°$ range with a step size of 0.01°. Scanning electron microscopy (SEM) images were obtained with HITACHI-S4100 apparatus operated at 20 kV.

Adsorption-desorption isotherms of nitrogen at –196 °C were measured with an automatic adsorption device (NOVA-1000 Gas Sorption analyzer) in order to determine surface area and total pore volume. The surface area of the obtained CES adsorbent was determined by Brunauer-Emmett-Teller (BET) method.

The pH was measured by a CrisonBasic 20+ pH-meter. The pH drift method was used to measure the pH zero point charge (pH$_{ZPC}$) of CES adsorbent as described in reference[23].

Adsorption experiments

Adsorption experiments were conducted with 50 mL of dye solution with a certain initial concentration in a beaker of 100 mL. Batch adsorption of Rhodamine B and Alizarin Red S dyes onto CES adsorbent was investigated in aqueous solutions by varying experimental conditions, such as adsorbent dosage (50 mg – 200 mg), initial dye concentration (20 mg L^{-1} – 50 mg L^{-1}), pH (2 – 12), and temperature (303 K – 323 K). Each experiment was repeated three times to find the average.

The removal (R) percentage and the amount adsorbed q_e (mg g^{-1}) of each dye was calculated using the following equations:

$$R = \left(\frac{\gamma_0 - \gamma_e}{\gamma_0} \right) \cdot 100 \tag{1}$$

$$q_e = (\gamma_0 - \gamma_e) \cdot \left(\frac{V}{m} \right) \tag{2}$$

where γ_0 and γ_e are the initial and the equilibrium concentrations of dye solutions (mg L^{-1}), respectively, whereas V and m are the volume of the solution (L) and the amount of used adsorbent (g), respectively.

Desorption and regeneration experiments

The reuse of the CES was considered in consecutive sorption-desorption cycles. For the desorption experiments, previously adsorbed dyes on CES were transferred to a flask containing 100 mL of desorbing agent, such as HCl (0.1 M), NaOH (0.1 M), and distilled water. The mixture was shaken at 100 rpm using a shaker (Innova 2300, New Brunswick, USA) at room temperature for 1 hour. In the regeneration experiment, the dye-loaded adsorbent that was eluted by the desorbing agents was thoroughly washed three times with deionized water to remove any traces of desorbing agent, and then mixed again with dye-loaded wastewater for the next adsorption cycle. This procedure was used for three consecutive cycles.

Results and discussion

Characterization of CES adsorbent

In order to study the surface of CES adsorbent, elemental analysis of obtained support was achieved by chemical composition using XRF. The results are given in Table 2.

The results indicated that CES was composed mainly of Ca. Other elements were found in lower percentage (Mg, Si, Na, P, Al, and Cl).

Fig. 1 shows the XRD spectrum of CES adsorbent. Evidently, a main peak appeared at 2θ = 34.13°. Furthermore, the spectrum shows several other small peaks at 2θ = 18.07°, 23.08°, 28.72°, 29.43°, 36.03°, 39.47°, 48.55°, 50.85°, 57.48°, 60.74°, 62.62°, 64.30°, 71.80°, and 81.88°, which confirms the presence of calcite and portlandite. Analysis of FT-IR spectrum of CES adsorbent, as shown in Fig. 2, resulted in some bands at 3600 cm^{-1} that were assigned to –OH stretching modes, and stretching and folding of carbonate group were assigned to peaks at 1500 cm^{-1} and 865 cm^{-1}. The

Table 2 – *Chemical composition of CES adsorbent by XRF*

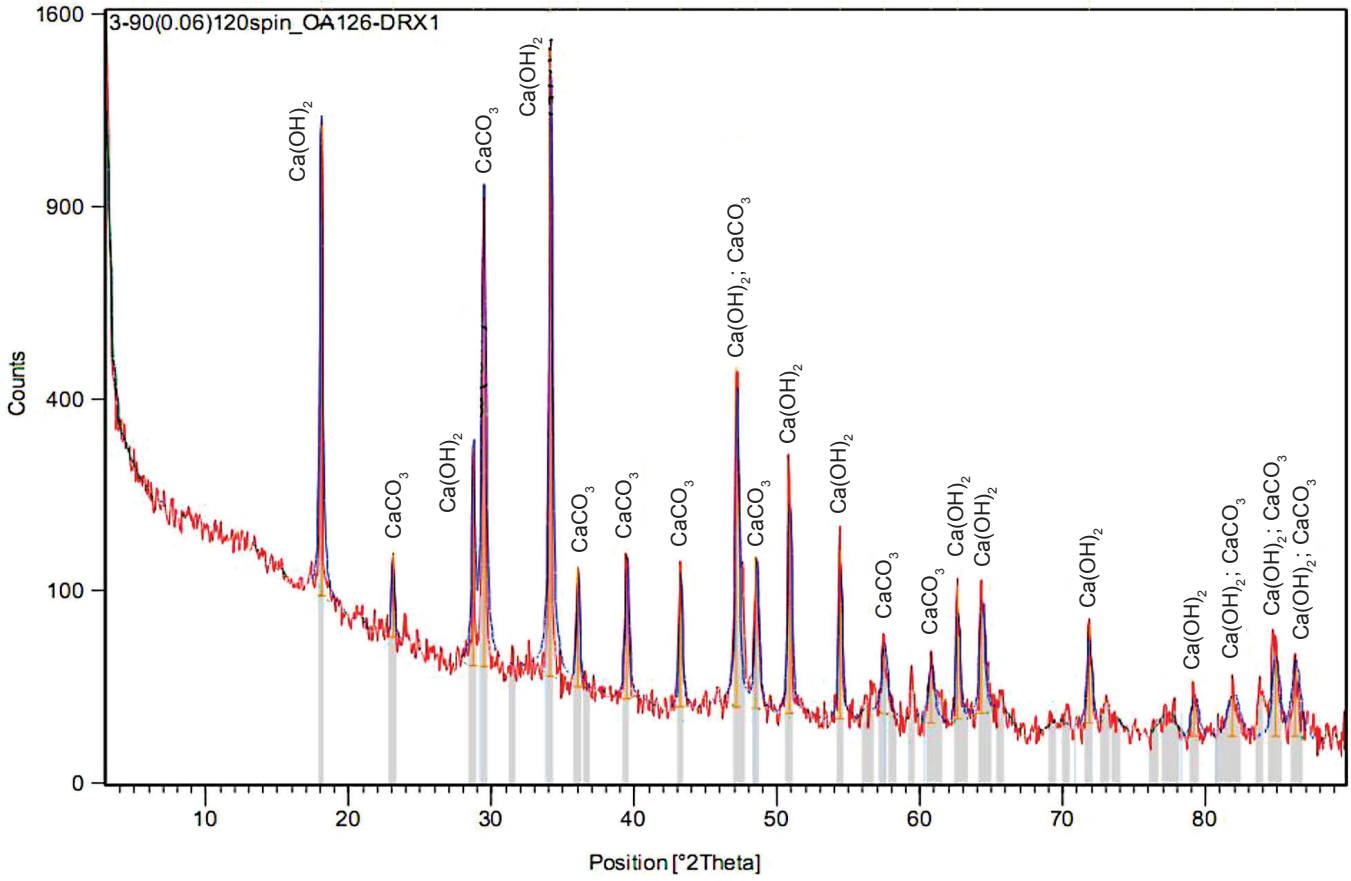| Chemical element	Percentage content (%)
Ca	61.95
Mg	0.79
Si	0.65
Na	0.64
P	0.47
Al	0.17
Cl	0.12

F i g. 1 – *XRD spectrum of CES adsorbent*
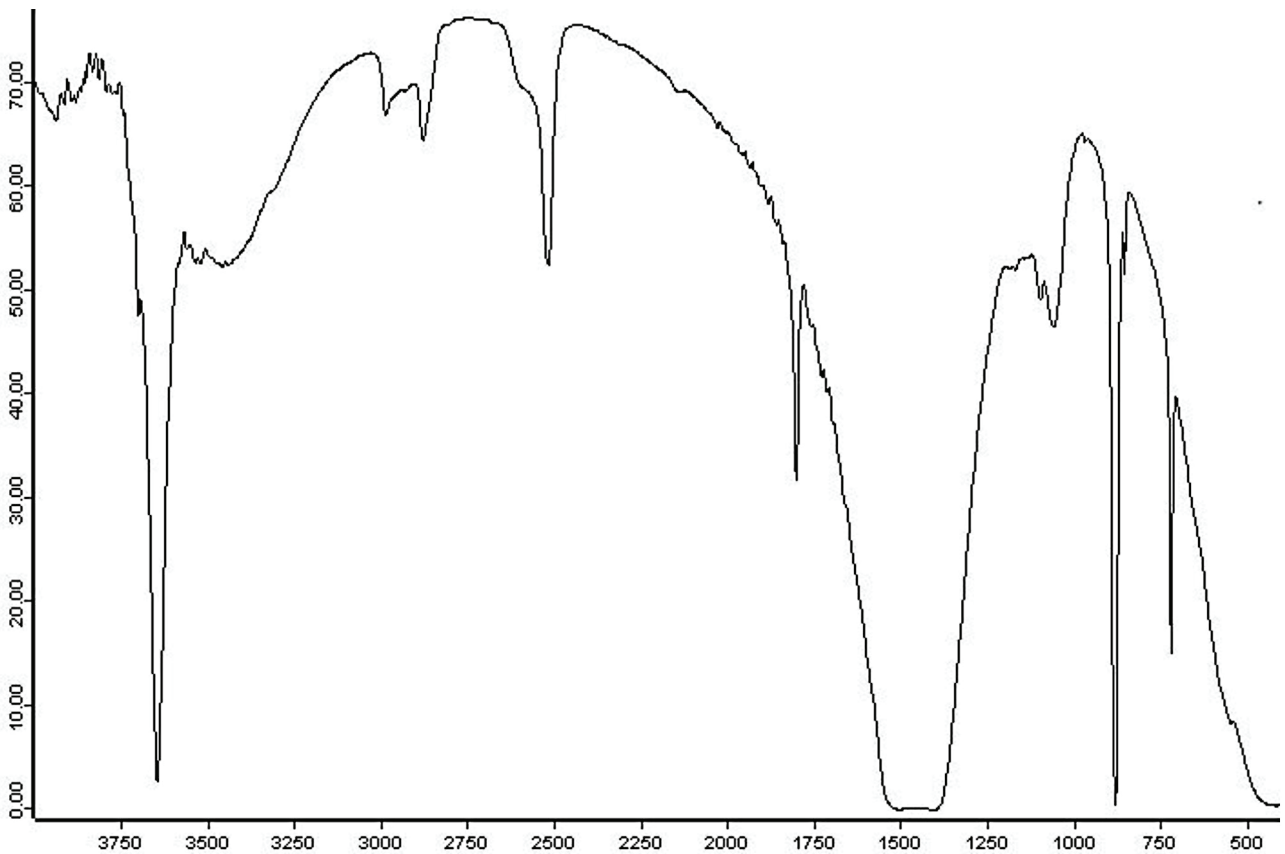
F i g. 2 – *IR spectrum of CES adsorbent*

a) 400 x   **b) 2000 x**
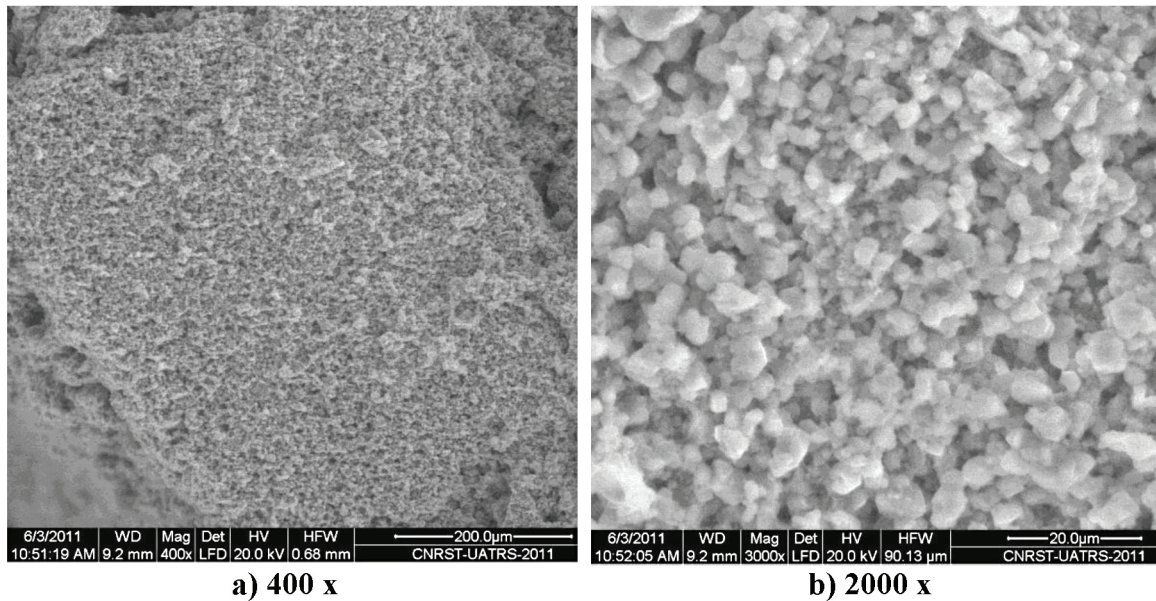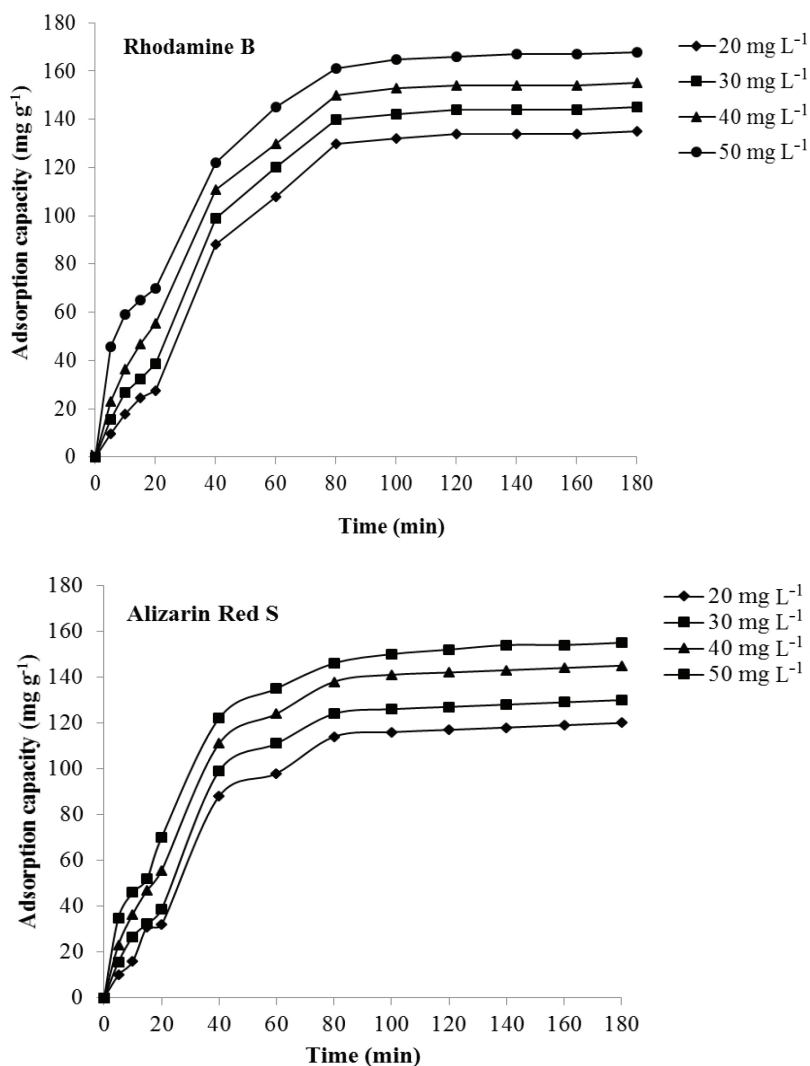
F i g . 3 – *SEM photographs of CES adsorbent*

F i g . 4 – *Effect of dye concentration on the adsorption capacity (γ_0 = 20 – 50 mg L^{-1}, adsorbent dosage: 150 mg, temperature: 25 °C)*

surface morphology of CES adsorbent observed by SEM, shown in Fig. 3, indicated that it consisted of tiny particles of calcite of various sizes. The specific surface area of the CES adsorbent calculated by the BET (Brunauer-Emmett-Teller) method was 62.42 m² g^{-1}.

Effect of contact time and concentration dye on the removal efficiency onto CES adsorbent

The effect of contact time and initial dye concentration on adsorption capacity at different initial concentrations of Rhodamine B and Alizarin Red S is shown in Fig. 4. As indicated in this figure, the adsorption capacity increased with contact time, and reached equilibrium in 2 hours; however, the increase was relatively higher during the first 40 minutes. Rapid increase in adsorption during the initial stage may presumably be due to the availability of vacant active sites on the surface of each dye. The slow increase at the later stages was due to the diffusion of dyes into the pores of CES adsorbent because of occupation of external sites. The adsorption capacity increased with dye concentration at any dye-adsorbent contact time. The values of adsorption capacity for a contact time of 180 minutes are shown in Fig. 5 against the equilibrium dye concentration for different initial dye concentrations. Furthermore, Fig. 5 indicates that the equilibrium adsorption capacity increases with increasing equilibrium dye concentration.
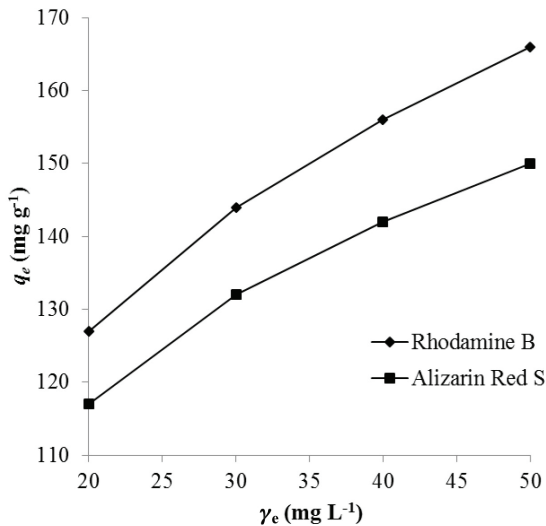
F i g . 5 – *Effect of equilibrium concentration of each dye on adsorption capacity ($\gamma_0 = 40$ mg L^{-1}, adsorbent dosage: 150 mg, temperature: 25 °C, contact time 3 h)*
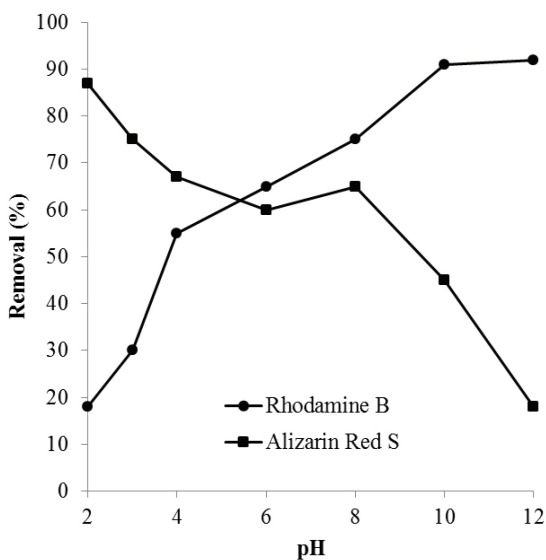

F i g . 6 – *Effect of pH on the dye removal onto CES adsorbent ($\gamma_0 = 40$ mg L^{-1}, adsorbent dosage: 500 mg, temperature: 25 °C)*
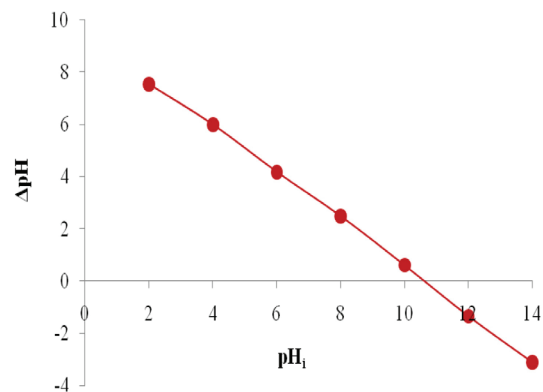

F i g . 7 – *Determination of pH$_{ZPC}$ of CES adsorbent*

Effect of pH on the removal efficiency of both dyes onto CES adsorbent

Fig. 6 illustrates results of the experiments. The removal performance of Rhodamine B increased from 18 % to 91 % when pH varied from 2 to 10. This increase can be explained by the fact that pH$_{ZPC}$ is equal to 10.2 (see Fig. 7), suggesting that the surface of CES adsorbent is positively charged under pH$_{ZPC}$ and negatively charged above pH$_{ZPC}$. This result can be explained by the fact that positive charges on the surface of CES adsorbent are completely neutralized by increasing pH (basic), which makes the surface negatively charged and subsequently promotes the adsorption of Rhodamine B as a cationic dye onto CES adsorbent. Such behavior has been already described with cationic dye in a previous research paper[24].

An opposite result was obtained with Alizarin Red S: its removal percentage decreased from 87 % to 18 % when pH increased from 2 to 10. This behavior is explained by having the surface of CES adsorbent charged positively, allowing a significant retention of a negatively charged Alizarin Red S under acidic conditions. Above pH$_{ZPC}$, the capacity adsorption will be reduced since there will be a repulsion of charge between CES adsorbent and Alizarin Red S.

For the following studies, we chose a basic pH above 10 for the adsorption of Rhodamine B, and acidic pH around 2 for the adsorption of Alizarin Red S.

Effect of adsorbent dosage on the dye removal onto CES adsorbent

Fig. 8 shows the variation of removal percentage and adsorption capacity compared to CES adsorbent dosage. It has been observed that R % increased for each dye (Rhodamine B or Alizarin Red S) when the CES adsorbent dosage increased from 50 mg to 200 mg. The adsorption saturation was reached at CES adsorbent dosage above 200 mg, and this amount of adsorbent was chosen for further studies. The increase in R % is due to increase in surface area and the availability of more binding sites for adsorption. The decrease in adsorption capacity with increasing adsorbent dosage might be due to interaction of adsorbent particles, like aggregation or agglomeration, which resulted with a decrease in the specific surface area.

Effect of CES adsorbent particle size on dye removal

Adsorption of Rhodamine B and Alizarin Red S onto CES adsorbent was studied using three different size fractions of adsorbent particles (75 – 100 µm,
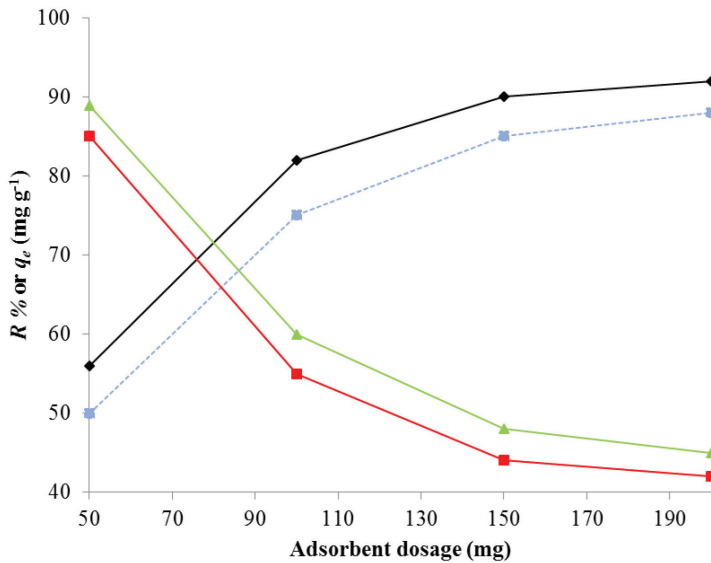
Fig. 8 – *Effect of adsorbent dosage on the removal % and adsorption capacity (γ_0 = 20 mg L^{-1}, adsorbent dosage: 50 – 200 mg, temperature: 25 °C, contact time 3 h)* ◆ – R % of Rhodamine B; ✖ – R % of Alizarin Red S; ▲ – q_e of Rhodamine B; ■ – q_e of Alizarin Red S
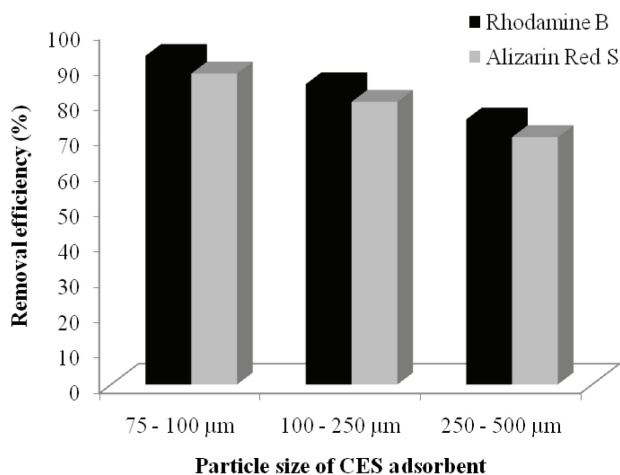

Fig. 9 – *Effect of CES adsorbent particle size on dye removal efficiency (γ_0 = 20 mg L^{-1}, adsorbent dose 150 mg, temperature 25 °C, contact time 3 h)*

100 – 250 μm, and 250 – 500 μm). Fig. 9 shows the effect of particle size on the removal efficiency of Rhodamine and Alizarin Red S. As illustrated in Fig. 9, whatever the nature of the dye, the removal efficiency decreased with increasing particle size. For Rhodamine B, removal efficiency decreased from 93 % to 75 % when increasing particle size range. Furthermore, for Alizarin Red S, it decreased from 88 % to 72 %. This is because smaller particle size provides large specific surface area for adsorption, which results in higher dye removal. In this case, we chose the range 75 – 100 μm particle size of CES adsorbent for further study.

Adsorption kinetics study

The adsorption process of Rhodamine B and Alizarin Red S onto CES adsorbent was tested against the pseudo-first-order, pseudo-second-order, and intra-particle diffusion kinetic model.

The pseudo-first-order kinetic model was widely used to predict the sorption kinetics[25,26] and was expressed as:

$$\log\left(q_e - q_t\right) = \log q_e - k_1 t \tag{3}$$

where, q_e and q_t (mg g^{-1}) are the amounts adsorbed at equilibrium and at any time, respectively, t (min) is time, and k_1 (min^{-1}) is the adsorption rate constant. The linear plot of $\log(q_e - q_t)$ versus t gives a slope of k_1 and intercept of $\log q_e$.

The values of k_1 and R^2 obtained from the plots for adsorption of Rhodamine B and Alizarin Red S dyes onto CES adsorbent are reported in Table 3. It was observed that the R^2 values obtained for the pseudo-first-order model showed no consistent trend. However, the experimental q_e values did not match the calculated values obtained from the linear plots. This showed that the adsorption of Rhodamine B and Alizarin Red S dyes onto the adsorbent did not follow a pseudo-first-order kinetic model.

The pseudo-second-order equation established by Ho and McKay[27] predicts the behavior over the whole range of adsorption, and is expressed as follows:

$$\frac{t}{q_t} = \frac{1}{k_2 q_e^2} + \frac{1}{q_e} t \tag{4}$$

The adsorption rate constant is k_2 (g mg^{-1} min^{-1}), and the linear plot of t/q_t vs t gave $1/q_e$ as the slope, and $\dfrac{1}{k_2 q_e^2}$ as the intercept. As illustrated in Table 3, all the R^2 values obtained from the pseudo-second-order model (see Fig. 10) were close to one, and the agreement between the calculated and experimental q_e values for Rhodamine B and Alizarin Red S dyes was quite good. This showed that the model could be applied for the entire adsorption process, and confirmed that the sorption of Rhodamine B and Alizarin Red S onto CES adsorbent followed the pseudo-second-order kinetic model.

The kinetics of diffusion was also tested against the intraparticle diffusion model[28] using the following equation:

$$q_t = k_{pi} \sqrt{t} + C_i \tag{5}$$

where, k_{pi} (mg g^{-1} min$^{-1/2}$), the rate parameter of stage i, is obtained from the slope (straight line) of q_t versus $t^{1/2}$. C_i represents the boundary layer effect, meaning that the larger the intercept, the greater the

Table 3 – *Kinetic data for the adsorption of Rhodamine B and Alizarin Red S onto CES adsorbent*

Dye	γ_0 (mg L^{-1})	$q_{e,exp}$ (mg g^{-1})	Pseudo-first-order			Pseudo-second-order		
			k_1 (min^{-1})	$q_{e,cal}$ (mg g^{-1})	R^2	k_2 (g mg^{-1} min^{-1})	$q_{e,cal}$ (mg g^{-1})	R^2
Rhodamine B	20	16.58	0.014	9.54	0.865	0.023	15.98	0.996
	30	27.36	0.018	15.26	0.921	0.034	26.45	0.998
	40	35.42	0.021	22.54	0.897	0.068	35.18	0.999
	50	48.36	0.023	32.41	0.915	0.078	49.23	0.999
Alizarin Red S	20	18.56	0.017	10.12	0.894	0.021	17.56	0.998
	30	28.54	0.019	15.12	0.875	0.054	27.69	0.999
	40	37.25	0.022	23.58	0.854	0.082	37.98	0.998
	50	49.05	0.025	29.58	0.912	0.095	49.56	0.999

Table 4 – *Data of intraparticle diffusion model for the adsorption of dye onto CES adsorbent*

| Dye	γ_0 (mg L^{-1})	Intraparticle diffusion model								
		k_{p1} (mg g^{-1} min$^{-1/2}$)	k_{p2} (mg g^{-1} min$^{-1/2}$)	k_{p3} (mg g^{-1} min$^{-1/2}$)	C_1	C_2	C_3	$(R_1)^2$	$(R_2)^2$	$(R_3)^2$
Rhodamine B	20	1.82	0.87	0.12	0	0.40	0.18	0.958	0.995	0.975
	30	2.52	0.94	0.18	0	1.20	0.24	0.987	0.992	0.994
	40	3.86	1.31	0.86	0	1.35	0.38	0.926	0.996	0.996
	50	5.15	2.34	1.05	0	2.14	0.75	0.9475	0.994	0.995
Alizarin Red S	20	1.45	0.78	0.09	0	0.31	0.15	0.921	0.992	0.992
	30	2.34	0.88	0.11	0	1.14	0.18	0.963	0.991	0.994
	40	3.76	1.15	0.75	0	1.22	0.32	0.985	0.998	0.997
	50	4.87	1.98	0.88	0	1.75	0.65	0.9141	0.994	0.994
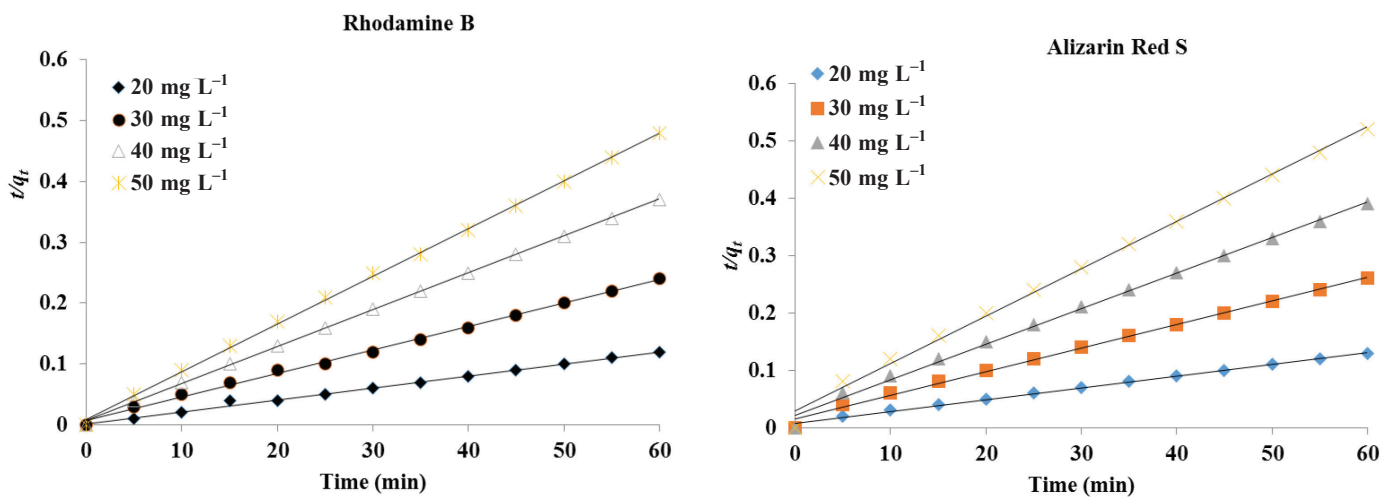
Fig. 10 – *Plot of curves corresponding to equation of pseudo–second–order kinetics for the adsorption of Rhodamine B and Alizarin Red S onto CES adsorbent*

Table 5 – *Isotherms data for the adsorption of Rhodamine B and Alizarin Red S dyes onto CES adsorbent at different temperatures*

Equations	Parameters	Rhodamine B			Alizarin Red S		
		303 K	313 K	323 K	303 K	313 K	323 K
Langmuir	K_L (L mg^{-1})	0.075	0.061	0.047	0.055	0.052	0.042
	C_m (mg g^{-1})	175.58	168.25	159.74	156.56	157.06	152.75
	R^2	0.997	0.999	0.997	0.999	0.998	0.998
Freundlich	K_F (mg g^{-1}) (L mg^{-1})$^{1/n}$	12.23	9.89	8.52	8.57	8.67	8.12
	n	2.45	2.32	2.18	1.78	1.68	1.57
	R^2	0.989	0.979	0.991	0.978	0.969	0.985
Temkin	K_T (L mg^{-1})	0.854	0.715	0.597	0.725	0.635	0.546
	B	17.12	17.34	17.76	15.24	15.45	15.78
	b_T (kJ mol^{-1})	0.147	0.150	0.151	0.165	0.168	0.170
	R^2	0.996	0.998	0.996	0.998	0.997	0.995
Dubinin-Radushkevich	q_S (mg g^{-1})	75.25	68.56	55.26	45.23	47.58	52.64
	E (kJ mol^{-1})	0.56	0.45	0.38	0.85	0.95	0.78
	R^2	0.895	0.799	0.892	0.875	0.759	0.854

contribution of the surface sorption in the rate-controlling step. The linearity of q_t versus $t^{1/2}$ confirms that the intraparticle diffusion is occurring, and the rate-limiting process is only due to the intraparticle diffusion if the plot passes through origin.

The values of k_{pi}, C_i and R^2 obtained for the three regions from the plots are given in Table 4, which shows that the k_p values for the three regions increase with increase in dye initial concentration. The result revealed that an increase in adsorbate concentration resulted in an increase in the driving force, which led to an increase in every dye diffusion rate. It was observed that the values of intercept increase are correlated to the increase in initial dye concentration from 20 to 50 mg L^{-1}, indicating the increase in the thickness of the boundary layer.

Adsorption isotherms study

In order to optimize the adsorption process, it is essential to describe the quantity adsorbed by a given amount of adsorbent. The equilibrium data was analyzed using Langmuir, Freundlich, Temkin and Dubinin-Radushkevich isotherms.

If the sorption takes place at specific homogeneous sites within the adsorbent, the Langmuir isotherm[29] may be considered, as expressed by the following formula:

$$\frac{\gamma_e}{q_e} = \frac{\gamma_e}{C_m} + \frac{1}{K_L C_m} \qquad (6)$$

where, γ_e (mg L^{-1}) is the equilibrium concentration of the adsorbent, and q_e (mg g^{-1}) is the amount adsorbed at equilibrium, C_m (mg g^{-1}) and K_L (L mg^{-1}) are constants related to adsorption capacity and energy of adsorption, respectively. The value of C_m and K_L can be determined from the slope and the intercept of the γ_e/q_e *vs* γ_e linear plot. Langmuir constants K_L and C_m are calculated from plots and are given in Table 5.

For Rhodamine B and Alizarin Red S dyes, values of C_m decreases with increase in temperature, suggesting the exothermic nature of adsorption processes.

The essential characteristic of the Langmuir isotherm can be expressed in terms of dimensionless equilibrium parameter[30] such as separation factor (R_L) used in the following equation:

$$R_L = \frac{1}{1 + K_L \gamma_0} \qquad (7)$$

where γ_0 (mg L^{-1}) is the initial dye concentration. The value of the parameter R_L indicates the nature of the adsorption processes. $R_L > 1$ for unfavorable adsorption, $R_L = 1$ for linear adsorption, $0 < R_L < 1$ for favorable adsorption, and $R_L = 0$ for favorable and irreversible adsorption.

Fig. 11 represents all calculated values of R_L versus temperature (303, 313, and 323 K) and Rhodamine B and Alizarin Red S dye concentrations (20, 30, 40, and 50 mg L^{-1}). Thus, all values of R_L were found between 0 and 1, suggesting that the adsorption of Rhodamine B and Alizarin Red S dyes onto CES adsorbent was favorable.

Freundlich isotherm is derived by assuming a heterogeneous surface with a non-uniform distribution of adsorption enthalpy over the surface. The linear form of Freundlich equation can be expressed as:
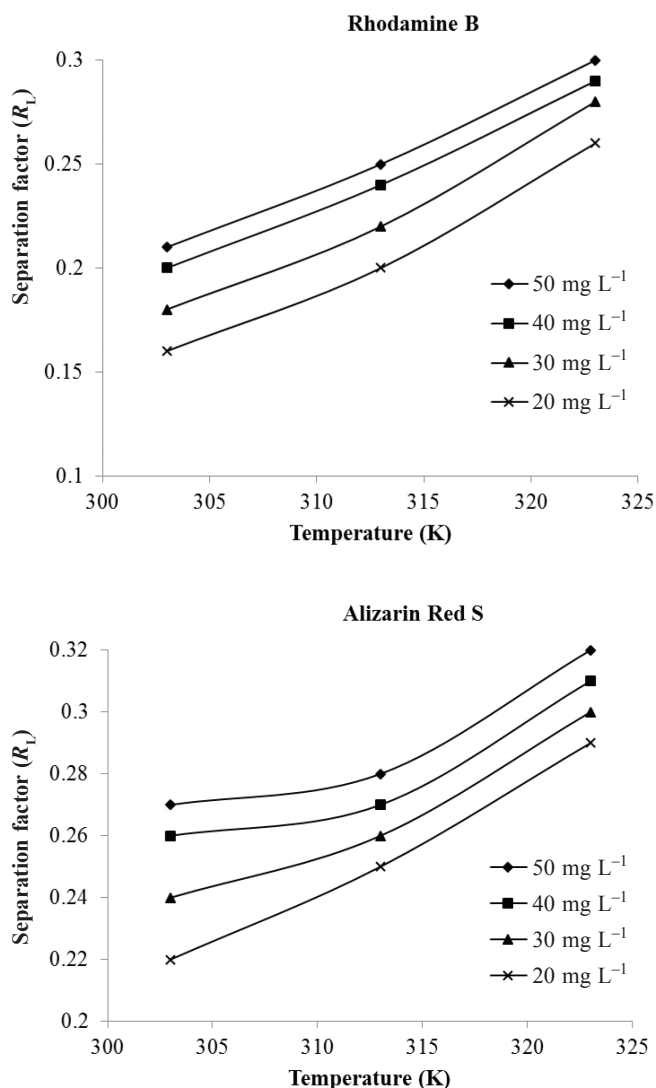
Rhodamine B

Alizarin Red S

F i g . 1 1 – *Effect of dye concentration and temperature on separation factor R_L*

$$\log q_{\text{e}} = \log K_{\text{F}} + \frac{1}{n} \log \gamma_{\text{e}} \qquad (8)$$

where, q_{e} is the amount adsorbed (mg g^{-1}), γ_{e} is the equilibrium concentration of the adsorbate (mg L^{-1}). K_{F} (mg g^{-1}) (L g^{-1})$^{1/n}$ and n, the Freundlich constants, are related to adsorption capacity and adsorption intensity, respectively. Freundlich constant n is a measure of the deviation from linearity of the adsorption, and if a value for n is equal to unity, the adsorption is linear. Value of n below unity implies that adsorption process is chemical, but if a value for n is above unity, adsorption is a favorable physical process[31].

Values of K_{F} and n, obtained from the slope and intercept of plot $\log q_{\text{e}}$ vs. $\log \gamma_{\text{e}}$, are shown in Table 5. Values of K_{F} decreased with the increase in temperature, showing the exothermic nature of adsorption process.

Temkin isotherm is derived by assuming that the heat of the adsorption of all molecules in the layer decreases linearly with coverage due to adsorbent-adsorbate interactions, and that the adsorption is characterized by uniform distribution of the binding energies, up to some maximum binding energy[32]. The linear form of Temkin isotherm can be expressed with the following formula:

$$q_{\text{e}} = B \ln K_{\text{T}} + B \ln \gamma_{\text{e}} \qquad (9)$$

where, γ_{e} (mg L^{-1}) is the concentration of the adsorbate at equilibrium, q_e (mg g^{-1}) is the amount of adsorbate adsorbed at equilibrium. The constant B can be expressed as follows:

$$B = \frac{RT}{b_{\text{T}}} \qquad (10)$$

where, T is the temperature (K), and R is the ideal gas constant (8.314 J mol^{-1} K^{-1}), K_{T} and b_{T} are the constants. A linear plot of q_{e} versus $\ln \gamma_{\text{e}}$ enables the determination of constants K_{T} and B. The constant b_{T} (kJ mol^{-1}) is related to the adsorption enthalpy, and K_{T} is the equilibrium binding constant (L mg^{-1}) corresponding to the maximum binding energy. The experiments on the adsorption of Rhodamine B and Alizarin Red S onto CES allowed for finding all the characteristic values of K_{T}, b_{T} and B, as shown in Table 5. In light of the results presented, low values of b_{T} for both dyes pointed to very weak interactions between Rhodamine B and Alizarin Red S and CES adsorbent, meaning that the adsorption of the studied dyes occurred by a physical process.

The Dubinin-Radushkevich (DR) isotherm is more general than the Langmuir isotherm because it does not consider a homogeneous surface or constant adsorption potential. It is used to distinguish between physical and chemical adsorption[33]. The linear equation for this isotherm is given as follows:

$$\ln q_{\text{e}} = \ln q_{\text{S}} - B \varepsilon^2 \qquad (11)$$

where:

$$= RT \ln \left(1 + \text{—} \right) \qquad (12)$$

where, q_{S} (mg g^{-1}) is the maximum amount adsorbed and is considered as DR constant, B is a constant giving the mean free energy E of the sorption per molecule of sorbate, and it is calculated by the following relation:

$$E = \frac{1}{\sqrt{2B}} \qquad (13)$$

Values of E less than 8 kJ mol^{-1} are characteristic for physisorption, and values of E between 8 and 16 kJ mol^{-1} are found for chemisorption. As maybe seen in Table 5, all the calculated values of E are below 8 kJ mol^{-1}, so it can be concluded that

the adsorption of both dyes occurs by physical processes. However, the relatively low values of R^2 point to the failure of DR isotherm to fairly describe the investigated adsorption phenomena.

Thermodynamics of adsorption

The values of the standard Gibbs free energy (ΔG^0) of adsorption for each temperature were calculated from the following equation:

$$\Delta G^0 = -RT \ln K_C \qquad (14)$$

where, R is the universal gas constant (8.314 J mol^{-1} K^{-1}), T is temperature, and K_C is the equilibrium constant that was calculated at each temperature using the following expression:

$$K_C = \frac{\gamma_S}{\gamma_e} \qquad (15)$$

where, γ_S and γ_e are the equilibrium concentrations on the adsorbent and the aqueous phase, respectively.

The enthalpy change (ΔH^0) and entropy change (ΔS^0) were calculated from the slope and intercept of the $\ln K_C$ versus $1/T$ based on the Van't Hoff equation:

$$\ln K_C = \left(\frac{\Delta S^0}{R}\right) - \left(\frac{\Delta H^0}{R}\right)\frac{1}{T} \qquad (16)$$

Table 6 depicts the thermodynamic data at temperatures and initial concentrations for the adsorptive removal of Rhodamine B and Alizarin Red S from aqueous solutions onto CES adsorbent. From Table 6, the negative values of ΔG^0 indicate a spontaneous and favorable adsorption process at all studied temperatures and initial concentrations of both dyes Rhodamine B and Alizarin Red S, suggesting that the system required no energy input from outside. For a given concentration of Rhodamine B or Alizarin Red S, ΔG^0 values increased with increasing temperature. Furthermore, values of ΔG^0 increased slightly as the initial Rhodamine B or Alizarin Red S concentration in-
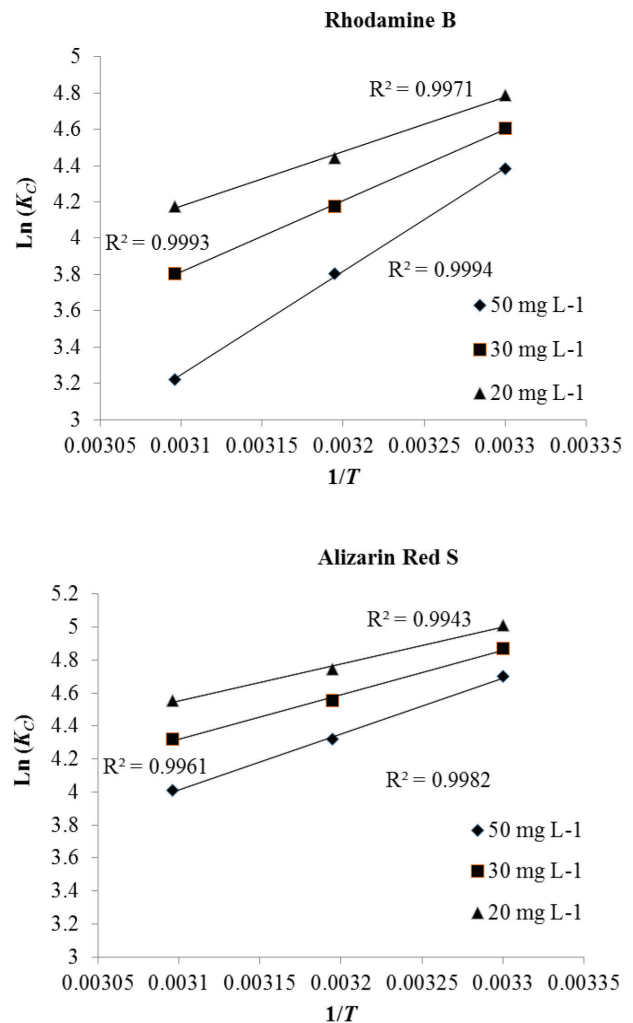

Fig. 12 – *Plots of ln(K_C) versus 1/T for the adsorption of Rhodamine B and Alizarin Red S onto CES adsorbent*

creased from 20 to 50 mg L^{-1}, indicating a more favorable adsorption of both dyes at lower dye concentration. The low negative values of ΔG^0 ranging from –20 to 0 kJ mol^{-1} suggest that the dominant adsorption mechanism was physisorption for the removal of Rhodamine B and Alizarin Red S onto CES adsorbent from aqueous solutions. As for the Van't Hoff plot, shown in Fig. 12, the regression

Table 6 – *Thermodynamic data for the adsorption of Rhodamine B and Alizarin Red S onto CES adsorbent at different temperatures*

Dye	γ_0 (mg L^{-1})	K_C 303 (K)	K_C 313 (K)	K_C 323 (K)	ΔG^0 (kJ mol^{-1}) 303 (K)	ΔG^0 (kJ mol^{-1}) 313 (K)	ΔG^0 (kJ mol^{-1}) 323 (K)	ΔH^0 (kJ mol^{-1})	ΔS^0 (J mol^{-1} K^{-1})
	20	120	85	65	–12.06	–11.56	–11.21	–24.97	–42.68
Rhodamine B	30	100	65	45	–11.60	–10.86	–10.22	–32.50	–69.03
	50	80	45	25	–11.04	–9.91	–8.64	–47.31	–119.61
	20	150	115	95	–12.62	–12.35	–12.23	–18.61	–19.84
Alizarin Red S	30	130	95	75	–12.26	–11.85	–11.59	–22.40	–33.55
	50	110	75	55	–11.84	–11.23	–10.76	–28.22	–54.13
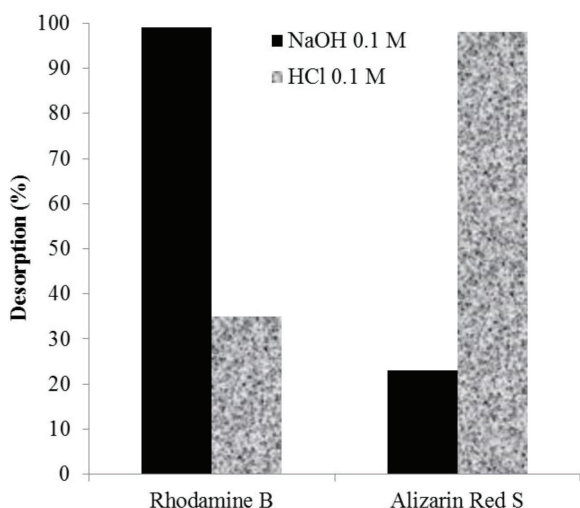
Fig. 13 – *Desorption study of Rhodamine B and Alizarin Red S onto CES adsorbent*

Fig. 14 – *Effect of number of cycle runs for the reusability of CES adsorbent*

coefficient (R^2) of the plots of $\ln K_C$ versus $1/T$ were close to one for all initial Rhodamine B and Alizarin Red S concentrations, indicating that the estimated values of ΔH^0 and ΔS^0 were reliable. As maybe be seen in Table 6, the negative values of ΔH^0 are due to the exothermic nature of the adsorption of Rhodamine B and Alizarin Red S onto CES adsorbent. Please note that similar results with negative ΔH^0 values were obtained by other studies, and were interpreted in terms of exothermic adsorption for anionic and cationic dyes[34,35].

The magnitude of enthalpy change can be used to classify the type of adsorbent-adsorbate interaction, and according to ΔH^0 values for Rhodamine B and Alizarin Red S obtained in this study, the adsorption of both dyes onto CES adsorbent was due to physical adsorption, suggesting weak interactions between CES adsorbent and chosen dye.

The negative values of ΔS^0 were very low, and pointed to increased ordering at the solid-liquid interface during the adsorption of dye onto CES adsorbent (see Table 6); the extent or ordering was larger for higher dye concentrations. The results also suggested that the enthalpy change ΔH^0 contributed more to the negative values of ΔG^0 than the corresponding entropy change ΔS^0. This suggested that the adsorption of dyes onto CES adsorbent was an enthalpy-controlled process.

Desorption, adsorbent regeneration, and adsorbent comparison

In order to regenerate the CES adsorbent for further use, it is important to study the desorption process as well. In this case, two different desorption agents were selected: NaOH 0.1 M and HCl 0.1 M. The results of this study are shown in Fig. 13. The result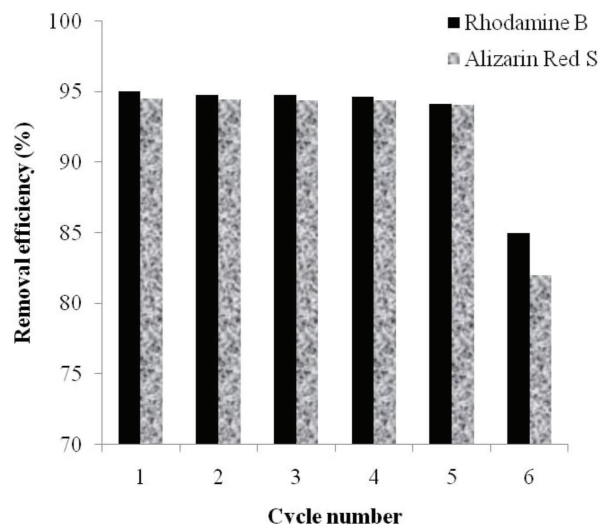s show that NaOH 0.1 M is a better de-sorption agent for Rhodamine B (giving 99 % desorption), and HCl 0.1 M is a better desorption agent for Alizarin Red S (giving desorption near 98 %). As shown in Fig. 14, the removal efficiency % decreased for each new cycle after regeneration, and after a sequence of six cycles, the Rhodamine B desorption efficiency decreased from 95 % to 85 %, and that of Alizarin Red S from 94 % to 82 %. The overall loss in removal efficiency for Rhodamine B was below 10 % and for Alizarin Red S below 13 %. Therefore, CES adsorbent could be used for five cycles of adsorption of Rhodamine B and Alizarin Red S.

Table 7 – *Comparison of adsorption capacities for Rhodamine B and Alizarin Red S on various adsorbents*

Dye	Adsorbent	q_e (mg g^{-1})	Reference
Rhodamine B	Coconut coir pith	14.9	36
	Rice husk	185.9	42
	Baker's yeast	25	43
	Scrap tires	307.2	41
	Tannery waste	250	40
	Bagasse pith	198.6	37
	Jute stick	87.7	39
	Eggshells	175.58	This study
Alizarin Red S	Olive stone	16	21
	Gold nanoparticles	123.4	22
	Mustard husk	6.4	20
	Chitosan	43.08	38
	Mussel shells	39.65	10
	Eggshells	156.56	This study

Table 7 summarizes the adsorbents applied for the removal of Rhodamine B and Alizarin Red S from aqueous solution. According to the results of this study, CES adsorbent can be used for the removal of dies with satisfactory results in comparison to adsorbents studied earlier.

Conclusion

Removal of Rhodamine and Alizarin Red S dyes was successfully achieved using treated eggshell waste. Kinetic study showed that adsorption of the two dyes followed pseudo-second-order kinetics. Furthermore, adsorption was best described by Langmuir isotherm. In addition, thermodynamic study showed that adsorption of Rhodamine B and Alizarin Red S was feasible, spontaneous, and exothermic in nature.

As a result, it may be concluded that CES adsorbent is an effective adsorbent for the removal of Rhodamine B and Alizarin Red S from aqueous solution. Moreover, CES adsorbent is cheap and widely available. Taking into consideration that it is a waste product, its usage can resolve some waste management issues as well.

References

1. *Fontana, K. B., Chaves, E. S., Sanchez, D. S., Watanabe, E., Pietrobelli, J., Lenzi, G.,* Textile dye removal from aqueous solutions by malt bagasse: Isotherm, kinetic and thermodynamic studies, Ecotox. Environ. Safe. **124** (2016) 329.
   doi: https://doi.org/10.1016/j.ecoenv.2015.11.012

2. *Shi, L., Wei, D., NgO, H. H., Guo, W., Wei, Q.,* Application of anaerobic granular sludge for competitive biosorption of methylene blue and Pb(II): Fluorescence and response surface methodology, Bioresour. Technol. **194** (2015) 297.
   doi: 10.1016/j.biortech.2015.07.029

3. *Deniz, F., Karaman, S.,* Removal of an azo-metal complex textile dye from colored aqueous solutions using an agro-residue, Microchem. J. **99** (2011) 296.
   doi: https://doi.org/10.1016/j.microc.2011.05.021

4. *Pathania, D., Sharma, A., Siddiqi, M.,* Removal of Congo Red dye from aqueous system using *Phoenix dactylifera* seeds, J. Mol. Liq. **219** (2016) 359.
   doi: https://doi.org/10.1016/j.molliq.2016.03.020

5. *Sonai, G., Guelli, S., Olievira, D., Souza, A.,* The application of textile sludge adsorbents for the removal the Reactive Red 2 dye, J. Environ. Manage. **168** (2016) 149.
   doi: https://doi.org/10.1016/j.jenvman.2015.12.003

6. *Kazemi, S. Y., Biparva, P., Ashtiani, E., Cerastoderma lamarcki* shell as natural, low cost and new adsorbent to removal of dye pollutant from aqueous solutions: Equilibrium and kinetic studies, Ecol. Eng. **88** (2016) 82.
   doi: https://doi.org/10.1016/j.ecoleng.2015.12.020

7. *Benkaddour, S., El Ouahabi, I., Hiyane, I., Essoufy, M., Driouich, A., El Antri, S., El Hajjaji, S., Slimani, R., Lazar, S.,* Removal of Basic Yellow 28 by biosorption onto watermelon seeds, Part I: The principal factors influencing by Plackett-Burman screening design, Surf. Interfaces **21** (2020) 100732.
   doi: https://doi.org/10.1016/j.surfin.2020.100732

8. *Hiyane, H., Benkadour, S., El Ouahabi, I., Slimani, R., Kartah, B., Aboudkhil, S., El Antri, S., Lazar, S.,* Calcined cow leather as a new low-cost biosorbent for copper (II), zinc (II) and nickel (II) ions removal from aqueous solution, Mor. J. Chem. **7** (2019) 683.
   doi: https://doi.org/10.48317/IMIST.PRSM/morjchem-v7i4.16140

9. *Slimani, R., Anouzla, A., Abrouki, Y., El Antri, S., Mamouni, R., Lazar, S., El Haddad, M.,* Removal of a cationic dye -Methylene Blue- from aqueous media by the use of animal bone meal as a new low cost adsorbent, J. Mater. Environ. Sci. **2** (2011) 77.

10. *El Haddad, M., Regti, A., Laamari, R., Slimani, R., Mamouni, R., El Antri, S., Lazar, S.,* Calcined mussel shells as a new and eco-friendly biosorbent to remove textile dyes from aqueous solutions, J. Taiwan. Inst. Chem. Eng. **45** (2014) 533.
    doi: https://doi.org/10.1016/j.jtice.2013.05.002

11. *Hachoumi, I., Benkaddour, S., El Ouahabi, I., Slimani, R., Cagnon, B., El Haddad, M., El Antri, S., Lazar, S., Ensis siliqua* shell for removal of Cu(II), Zn(II) and Ni(II) from aqueous solutions: Kinetics and isotherm model, Anal. Chem. Lett. **9** (2019) 50.
    doi: https://doi.org/10.1080/22297928.2019.1569555

12. *El Ouahabi, I., Slimani, R., Benkaddour, S., Hiyane, S., Cagnon, B., El Haddad, S., El Antri, S., Lazar, S.,* Adsorption of textile dye from aqueous solution onto a low cost conch shells, J. Mater. Environ. Sci. **9** (2018) 1987.

13. *Geng, J., Gu, F., Chang, J.,* Fabrication of magnetic lignosulfonate using ultrasonic-assisted *in situ* synthesis for efficient removal of Cr(VI) and Rhodamine B from wastewater, J. Hazard. Mater. **375** (2019) 174.
    doi: https://doi.org/10.1016/j.jhazmat.2019.04.086

14. *Sabarish, R., Unnikrishnan, G.,* Novel biopolymer templated hierarchical silicalite-1 as an adsorbent for the removal of Rhodamine B, J. Mol. Liq. **272** (2018) 919.
    doi: https://doi.org/10.1016/j.molliq.2018.10.093

15. *Zhang, Z., Chen, H., Wu, W., Pang, W., Yan, G.,* Efficient removal of Alizarin Red S from aqueous solution by polyethyleneimine functionalized magnetic carbon nanotubes, Bioresour. Technol. **293** (2019) 122100.
    doi: https://doi.org/10.1016/j.biortech.2019.122100

16. *Burakov, A., Neskoromnaya, E., Babkin, A.,* Removal of the Alizarin Red S anionic dye using graphenenanocomposites: A study on kinetics under dynamic conditions, Mater. Today-Proc. **11** (2019) 392.
    doi: https://doi.org/10.1016/j.matpr.2019.01.002

17. *Inyinbor, A. A., Adekola, F. A., Olatunji, G. A.,* Kinetics, isotherm, and thermodynamic modeling of liquid phase adsorption of Rhodamine B dye onto *Raphia hookeri* fruit epicarp, Water. Resour. Manag. **15** (2016) 14.
    doi: https://doi.org/10.1016/j.wri.2016.06.001

18. *Zamouche, M., Arris, S., Bencheikh, M.,* Removal of Rhodamine B from water by cedar cone: Effect of calcinations and chemical activation, Int. J. Hydrogen. Energ. **39** (2014) 1523.
    doi: https://doi.org/10.1016/j.ijhydene.2013.06.144

19. *Hou, M., Ma, C., Zhang, W., Tang, X., Fan, Y., Wan, H.,* Removal of Rhodamine B using iron-pillared bentonite, J. Hazard. Mater. **186** (2011) 1118.
doi: https://doi.org/10.1016/j.jhazmat.2010.11.110

20. *Goutam, R. K., Mudhoo, A., Chandra, M.,* Kinetic, equilibrium, thermodynamic studies and spectroscopic analysis of Alizarin Red S removal by mustard husk, J. Environ. Chem. Eng. **1** (2013) 1283.
doi: https://doi.org/10.1016/j.jece.2013.09.021

21. *Albadarin, A. B., Mangwandi, C.,* Mechanisms of Alizarin Red S and Methylene Blue biosorption onto olive stone by product: Isotherm study in single and binary systems, J. Environ. Manage. **164** (2015) 86.
doi: https://doi.org/10.1016/j.jenvman.2015.08.040

22. *Roosta, M., Ghaedi, M., Mohammadi, M.,* Removal of Alizarin Red S by gold nanoparticles on activated carbon combined with ultrasound device: Optimization by experimental design methodology, Powder. Technol. **267** (2014) 134.
doi: https://doi.org/10.1016/j.powtec.2014.06.052

23. *Foo, K. Y., Hameed, B. H.,* Potential of jackfruit peel as precursor for activated carbon prepared by microwave induced NaOH activation, Bioresour. Technol. **112** (2012) 143.
doi: https://doi.org/10.1016/j.biortech.2012.01.178

24. *Aboua, K. N., Abouet, Y. A., Yao, K. B., Goné, D. L., Trokourey, A.,* Investigation of dye adsorption onto activated carbon from the shells of Macoré fruit, J. Environ. Manage. **156** (2015) 10.
doi: https://doi.org/10.1016/j.jenvman.2015.03.006

25. *Hameed, B. H., Ahmad, A. L., Latiff, K. N. A.,* Adsorption of basic dye (Methylene Blue) onto activated carbon prepared from rattan sawdust, Dyes. Pigm. **75** (2009) 143.
doi: https://doi.org/10.1016/j.dyepig.2006.05.039

26. *Slimani, R., El Ouahabi, I., El Haddad, M., Regti, A., Laamari, R., El Antri, S., Lazar, S.,* Calcined eggshells as a new biosorbent to remove basic dye from aqueous solutions: Thermodynamics, kinetics, isotherms and error analysis, J. Taiwan. Inst. Chem. Eng. **45** (2014) 1578.
doi: https://doi.org/10.1016/j.jtice.2013.10.009

27. *Ho, Y. S., McKay, G.,* Pseudo-second-order model for sorption process, Process. Biochem. **34** (1999) 451.
doi: https://doi.org/10.1016/S0032-9592(98)00112-5

28. *Weber, W. J., Moris, J. C.,* Kinetics of adsorption on carbon from solution, J. Sanit. Eng. Div. **18** (1963) 31.

29. *Langmuir, I.,* The constitution and fundamental properties of solids and liquids. Part I, Solids, J. Am. Chem. Soc. **38** (1916) 2221.
doi: https://doi.org/10.1021/ja02268a002

30. *Zheng, H., Wang, Y., Zheng, Y., Zhang, H., Liang, S., Long, M.,* Equilibrium, kinetic and thermodynamic studies on the sorption of 4-hydroxyphenol on Cr-bentonite, Chem. Eng. J. **143** (2008) 117.
doi: https://doi.org/10.1016/j.cej.2007.12.022

31. *Freundlich, H. M. F.,* Über die Adsorption in Lösungen, Z. Phys. Chem. **57** (1906) 385.

32. *Temkin, M. J., Pyzhev, V.,* Kinetics of ammonia synthesis on promoted iron catalysts, Acta. Physicochim. U.R.S.S. **12** (1940) 217.

33. *Dubinin, M. M., Zaverina, E. D., Radushkevich, L. V.,* Sorption and structure of active carbons. I. Adsorption of organic vapors, Zh. Fiz. Khim. **21** (1947) 1351.

34. *El Haddad, M., Slimani, R., Mamouni, R., El Antri, S., Lazar, S.,* Removal of two textile dyes from aqueous solutions onto calcined bones, J. Assoc. Arab Univ. Basic Appl. Sci. **14** (2013) 51.
doi: https://doi.org/10.1016/j.jaubas.2013.03.002

35. *El Haddad, M., Slimani, R., Mamouni, R., Laamari, R., Rafqah, S., Lazar, S.,* Evaluation of potential capability of calcined bones on the adsorptive removal efficiency of safranin as cationic dye from aqueous solutions, J. Taiwan. Inst. Chem. Eng. **44** (2013) 13.
doi: https://doi.org/10.1016/j.jtice.2012.10.003

36. *Sureshkumar, M. V., Namasivayam, C.,* Adsorption behavior of Direct Red 12B and Rhodamine B from water onto surfactant-modified coconut coir pith, Colloid. Surf. A-Physicochem. Eng. Asp. **317** (2008) 277.
doi: https://doi.org/10.1016/j.colsurfa.2007.10.026

37. *Gad, H. M. H., El-Sayed, A. A.,* Activated carbon from agricultural by-products for the removal of Rhodamine-B from aqueous solution, J. Hazard. Mater. **168** (2009) 1070.
doi: https://doi.org/10.1016/j.jhazmat.2009.02.155

38. *Fan, L., Zhang, Y., Li, X., Luo, C., Lu, F., Qiu, H.,* Removal of alizarin red from water environment using magnetic chitosan with Alizarin Red as imprinted molecules, Colloid. Surface. B. **91** (2012) 250.
doi: https://doi.org/10.1016/j.colsurfb.2011.11.014

39. *Panda, G. C., Das, S. K., Guha, A. K.,* Jute stick powder as a potential biomass for the removal of congo red and rhodamine B from their aqueous solution, J. Hazard. Mater. **164** (2009) 374.
doi: https://doi.org/10.1016/j.jhazmat.2008.08.015

40. *Anandkumar, J., Mandal, B.,* Adsorption of chromium(VI) and Rhodamine B by surface modified tannery waste: Kinetic, mechanistic and thermodynamic studies, J. Hazard. Mater. **186** (2011) 1088.
doi: https://doi.org/10.1016/j.jhazmat.2010.11.104

41. *Li, L., Liu, S., Zhu, T.,* Application of activated carbon derived from scrap tires for adsorption of Rhodamine B, J. Environ. Sci. **22** (2010) 1273.
doi: https://doi.org/10.1016/S1001-0742(09)60250-3

42. *Ding, L., Zou, B., Gao, W., Liu, Q., Wang, Z., Guo, Y., Wang, X., Liu, Y.,* Adsorption of Rhodamine B from aqueous solution using treated rice husk – based activated carbon, Colloid. Surf. A-Physicochem. Eng. Asp. **446** (2008) 1.
doi: https://doi.org/10.1016/j.colsurfa.2014.01.030

43. *Yu, J., Li, B., Sun, X., Jun, Y., Chi, R.,* Adsorption of methylene blue and rhodamine B on baker's yeast and photocatalytic regeneration of the biosorbent, Biochem. Eng. J. **45** (2009) 145.
doi: https://doi.org/10.1016/j.bej.2009.03.007